Multivariate Resource Usage Prediction with Frequency-enhanced and Attention-assisted Transformer in Cloud Computing Systems

Jing Bi, *Senior Member, IEEE*, Haisen Ma, *Student Member, IEEE*, Haitao Yuan, *Senior Member, IEEE*, Rajkumar Buyya, *Fellow, IEEE*, Jinhong Yang, Jia Zhang, *Senior Member, IEEE*, and MengChu Zhou, *Fellow, IEEE*

***Abstract*—Resource usage prediction in cloud data centers is critically important. It can improve providers' service quality and avoid resource wastage and insufficiency. However, the time series of resource usage in cloud environments is characterized by multidimensional, nonlinear, and high-volatility characteristics. Achieving high-accuracy prediction for time series with such characteristics is necessary but difficult. Traditional prediction methods based on regression algorithms and recurrent neural networks cannot effectively extract non-linear features from datasets. Besides, many deep learning models suffer from gradient explosion or gradient vanishing during the training stage. Current commonly used prediction methods fail to uncover some vital information about the frequency domain features in the time series. To resolve these challenges, we design a Forecasting method based on the Integration of a Savitzky-Golay (SG) filter, a Frequency Enhanced Decomposed Transformer (FEDformer) model, and a Frequency-Enhanced channel Attention mechanism named FISFA. It adopts the SG filter to reduce noise and smooth sequences in the raw sequences of resources. Then, we develop a hybrid transformer-based model integrating FEDformer and the frequency-enhanced channel attention mechanism, effectively capturing the frequency domain patterns. Besides, a meta-heuristic optimization algorithm, *i.e.*, genetic simulated annealing-based particle swarm optimizer, is proposed to optimize key hyperparameters of FISFA. Then, FISFA predicts the future needs for multi-dimensional resources in highly fluctuating traces in real-life cloud environments. Experimental results demonstrate that FISFA achieves higher accuracy and performs more efficient prediction than several benchmark forecasting methods with realistic datasets collected from Alibaba and Google cluster traces. FISFA improves the prediction accuracy on average by 32.14%, 25.49%, and 27.71% over vanilla LSTM, Transformer, and Informer methods, respectively.**

***Index Terms*—Cloud computing, time series prediction, deep learning, frequency enhancement, SG filter**

I. Introduction

As companies and organizations increasingly rely on cloud computing infrastructure, cloud data centers (CDCs) are growing popular due to their high availability and flexibility [1], [2]. These CDCs provide a variety of software and hardware, including computing, storage, and network resources in a pay-as-you-go way [3]. Individuals or organizations can rent computing resources as cloud services according to their needs. Cloud service providers [4] can avoid wasting resources and save the cost of managing infrastructure. Current famous Internet companies like Google, Microsoft, and Amazon have almost countless computing devices. To maximize the utilization of these computing resources, they have established their CDCs. Their computing tasks generate resource usage time series, including CPU, memory, disk, network, and I/O [5]. However, the high volatility and nonlinearity of the time series may result in over or under provisioning of resources [6]–[8]. For example, simultaneously, a large influx of tasks can easily cause resource shortages [9]. During periods with a few tasks, such as midnight, idle server clusters can result in resource wastage. According to [10], the mean CPU utilization of the whole servers in Alibaba CDCs varies between 5% and 85%, showing considerable fluctuations. Thus, designing an accurate prediction method that can effectively extract relationships and features among multi-dimensional resource usage time series is critically important.

Time series prediction has attracted a considerable number of studies [11]. Traditional prediction approaches include linear regression [12] and AutoRegressive Integrated Moving Average (ARIMA) [13]–[15]. Nevertheless, when the regularity of the time series is not obvious, most of them cannot achieve the accurate prediction. In addition, these approaches fail to extract complicated characteristics and patterns of time

This work was supported in part by the National Natural Science Foundation of China under Grants 62173013 and 62073005, the Beijing Natural Science Foundation under Grants 4232049 and L233005, and the Fundamental Research Funds for the Central Universities under Grant YWF-23-03-QB-015. (Corresponding author: Haitao Yuan.)

J. Bi and H. Ma are with the School of Software Engineering in the Faculty of Information Technology, Beijing University of Technology, Beijing 100124, China. (e-mail: bijing@bjut.edu.cn; mahaisen@emails.bjut.edu.cn).

H. Yuan is with the School of Automation Science and Electrical Engineering, Beihang University, Beijing, China. (e-mail: yuan@buaa.edu.cn).

R. Buyya is with the Cloud Computing and Distributed Systems (CLOUDS) Lab, School of Computing and Information Systems, University of Melbourne, Melbourne, VIC 3010, Australia (e-mail: rbuyya@unimelb.edu.au).

J. Yang is with the CSSC Systems Engineering Research Institute in Beijing, China. (e-mail: yangjinhong.66@163.com).

J. Zhang is with the Department of Computer Science, Southern Methodist University, Dallas, TX 75206, USA. (e-mail: jiazhang@smu.edu).

M. Zhou is with the Department of Electrical and Computer Engineering, New Jersey Institute of Technology, Newark, NJ 07102, USA. (e-mail: zhou@njit.edu).

series datasets efficiently. Unlike the abovementioned methods, recurrent neural network (RNN) models have stronger sequence processing capabilities. Their variants [16]–[20] have been thoroughly employed for the time series prediction in the past few years. For example, long short-term memory (LSTM) is adopted to predict future short-term wind power in [16]. Gupta *et al.* propose a sparse Bidirectional LSTM (BiLSTM) network for future resource usage prediction. Saha *et al.* choose the LSTM-based encoder and decoder for the multi-step Internet traffic prediction.

However, they cannot efficiently capture long-term dependencies and association information among different dimensions in the time series. Currently, some studies [21], [25]–[28] have used transformer-based models to achieve the prediction. For example, a variant named multi-size patched spatial-temporal transformer is presented to achieve the urban crowd prediction in [21]. A non-autoregressive transformer-based model is designed for vehicle trajectory prediction. A variant that combines the transformer and the Markov-chain Monte Carlo algorithm is designed to predict electrical energy consumption. However, these studies cannot effectively extract the frequency domain information in the series. To solve the abovementioned challenges, we design a Forecasting method based on the Integration of a Savitzky-Golay (SG) filter [22], a Frequency Enhanced Decomposed Transformer (FEDformer) model [23], and a Frequency-Enhanced channel Attention mechanism (FECAM) [24], named FISFA for short. FISFA first adopts the SG filter to reduce noise and smooth the raw time series of resources. Then, FISFA adopts the FEDformer model to accurately predict resource usage time series by capturing their global features. In addition, FISFA adopts the FECAM module to improve the capability for extracting frequency features. Our key contributions are summarized as:

1) This work innovatively applies a noise reduction method of the filter of SG. It can smooth extreme points in the time series, highlight critical features of the data, and facilitate subsequent learning and extraction of features.
2) This work designs an improved transformer-based model integrating FEDformer and FECAM to achieve higher forecasting accuracy of resource usage series. The proposed method can learn frequency domain information and relationships among the multi-dimensional time series of resources.
3) This work designs a new hybrid metaheuristic algorithm, *i.e.*, Genetic Simulated annealing-based Particle Swarm Optimization (GSPSO) to optimize the setting of hyperparameters. GSPSO integrates quick convergence of particle swarm optimization (PSO), global search ability of simulated annealing (SA), and diversity of genetic algorithm (GA).

The rest of the paper is structured as follows. Section II discusses the related work. Section III describes the framework of FISFA. Experimental results are presented in Section IV. Section V concludes the paper along with a discussion on future work..

II. Related Work

Recent studies have proposed predicting computing resources. These prediction methods mainly include two kinds: classical and deep learning-based prediction methods.

A. Classical Time Series Prediction Methods

Traditional statistical analysis and regression methods are employed in resource usage forecasting in cloud computing. Gyeera *et al.* [29] adopt a Boosted Decision Tree (BDT) regression method in a realistic testbed in the Azure cloud. BDT performs better than other machine learning algorithms, such as stochastic gradient descent and ordinary least square linear regression. However, as an iterative algorithm, BDT requires a long training time. Zhang *et al.* [30] propose an XGBoost-based lane change prediction method with the realistic series data collected from autopilot vehicles. It has higher forecasting accuracy than adaptive boosting, gradient boosting trees, and random forest. However, the dataset used in this work is less volatile than the sequence of resources in CDCs. An integrated prediction method that combines Seasonal AutoRegressive Integrated Moving Average (SARIMA) and gradient BDT is designed in [31]. However, SARIMA suffers from significant errors in long-term prediction. Besides, it performs poorly in capturing non-linear characteristics of the sequence data. Shen *et al.* [32] present a support vector machine (SVM)-based transfer method for predicting rolling bearing remaining useful life. Yet, its dataset shows lower fluctuation than the resource usage series in real-life large-scale CDCs. Wang *et al.* [33] introduce an enhanced linear regression algorithm for the prediction of real-time CPU temperature of servers. However, it fails to capture certain potential features in the data, mainly when dealing with highly non-linear and non-stationary series. To achieve an online workload prediction framework, Kim *et al.* [34] propose an ensemble model using several traditional prediction methods, including linear regression, linear SVM, ARIMA, *etc*. It achieves higher accuracy than a single traditional forecasting method.

Above all, most classic time series forecasting models are based on statistical or regression models. These methods require apparent trends in the time series and perform poorly in long-term prediction. Unlike these methods, this work employs an improved transformer-based model, which can extract features from cloud environments' highly non-linear and variable computing resource usage data.

B. Deep Learning-based Prediction Methods

With the improvement of the computing power of servers, many studies utilize deep learning models for addressing time series prediction problems. Kumar *et al.* [35] propose a workload forecasting approach for requests for the industrial Internet of Things (IoT). This approach adopts deep autoencoders (DAEs) to predict the CPU cycles of cloud servers. However, DAEs train each layer individually in a layer-wise manner. It suffers from long training time and high computational complexity. Li *et al.* [36] introduce a Temporal Convolutional Network (TCN)-based prediction model for utility-scale photovoltaic forecasting. It captures spatial-temporal correlations to improve prediction accuracy for enormous intra-hour photovoltaic power. Wang *et al.* [37] design a prediction model that consists of a TCN layer and a Graph Convolution Network (GCN) layer for traffic datasets of geo-distributed data centers. Nevertheless, it mainly focuses on the temporal dependencies of the extracted series. A deep concatenated multi-layer perceptron [38] is proposed in an IoT network for fog sensor data prediction. However, the multi-layer perceptron network often yields inferior prediction outputs than standard LSTM models. Ruan *et al.* [39] present a feature-enhanced LSTM approach to extract the crucial sequence patterns in the cloud environment. However, LSTM [40] is an RNN-based model that fails to handle the gradient vanishing issue during the training process effectively. Its performance is unsatisfying for long-term prediction. The emergence of the transformer model has revolutionized the conventional use of RNN structures for processing sequence data. The model employs an encoder-decoder architecture and depends on an attention mechanism. Gao *et al.* [41] introduce a dual transformer model to predict both lane change intentions and trajectory projections of target vehicles. However, the trajectory dataset exhibits lower volatility than the workload data from CDCs. Furthermore, many variants of transformer-based models have been introduced and utilized in time series forecasting. Zhang *et al.* [42] propose an improved informer by a data augmentation approach for forecasting the deterioration of aircraft engines. However, the transformers perform better than RNNs in capturing long-term dependency in the time domain. These methods cannot effectively investigate the patterns in the frequency domain. Yet, the frequency domain information is crucial in forecasting data points in time series.

In summary, current deep learning methods mainly adopt RNNs and transformers for forecasting the time series. RNN-based methods fail to solve the problems of gradient vanishing and long-term prediction. Most transformer-based methods primarily focus on the temporal information within the time series while disregarding the crucial frequency domain information. Unlike previous studies, our work proposes a new method named FISFA that integrates the SG filter, FEDformer, and FECAM module for multi-dimensional prediction of the resource usage time series in CDCs. During the data preprocessing stage, the SG filter eliminates noises and outliers in the raw data. Then, the FEDformer with FECAM effectively captures the frequency domain information in the time series data, leading to a more accurate prediction.

III. Model Framework

The section describes the details of FISFA. First, our problem definition is shown in subsection III-A. Furthermore, we present the filter of SG in subsection III-B. Then, we describe FISFA in detail in subsection III-C. Finally, we present the details of the GSPSO used to optimize FISFA's hyperparameter setting. For clarity, Table I summarizes the main abbreviations in this work.

A. Problem Definition

This work chooses I to represent a multi-dimensional computing resource usage series in a CDC and $I{=}(I_1, I_2, \ldots, I_{t-1}, I_t)$. Previous t time slots are used to predict the values of computing resource usage at $t{+}1$. $\hat{y}_{t+1}$ denotes the final prediction value, which is obtained as:

$$\hat{y}_{t+1}{=}\mathrm{f}\left(I_1, I_2, \ldots, I_{t-1}, I_t\right). \quad (1)$$

The proposed method aims to reduce errors between the ground truth values and the predicted ones.

TABLE I
Abbreviation List

Abbreviation	Definition
CDCs	Cloud Data Centers
ARIMA	AutoRegressive Integrated Moving Average
SVM	Support Vector Machine
BDT	Boosted Decision Tree
RNN	Recurrent Neural Network
LSTM	Long Short-Term Memory
DAE	Deep AutoEncoder
GCN	Graph Convolution Network
TCN	Temporal Convolutional Network
SG	Savitzky-Golay filter
FEB	Frequency-Enhanced Block
FEA	Frequency-Enhanced Attention
DFT	Discrete Fouier Transform
DCT	Discrete Cosine Transform
FECAM	Frequency-Enhanced Channel Attention Mechanism
PSO	Particle Swarm Optimization
GSPSO	Genetic Simulated annealing-based PSO

B. Savitzky-Golay (SG) Filter

The SG filter [22] can decrease the noise of the time series through the least square polynomial smoothing method. Thus, we adopt it to extract the primary information in the preprocessing phase. It is processed by fitting successive subsets of each single-dimensional resource usage series with a low-degree polynomial.

I_t is the value (CPU or memory usage) in time slot t. $P_k{=}(p_{k-b}, \ldots, p_k, \ldots, q_{k+b})$, $k{\in}[b{+}1, t{-}b]$, which is a subsequence of I. Its width is $2b+1$. The SG filter adopts the following polynomial to fit it.

$$O(n){=}\sum_{r=0}^{R} a_r n^r \quad n{\in}[-b, b]. \quad (2)$$

where a_r denotes coefficient r of the polynomial, and R denotes a polynomial order. The fitting is achieved by minimizing the mean-squared error ϵ for each subsequence centered at 0. ϵ is defined as:

$$\epsilon{=}\sum_{n=-b}^{b}(O(n){-}p_{k+b})^2{=}\sum_{n=-b}^{b}(\sum_{r=0}^{R} a_r n^r{-}p_{k+b})^2. \quad (3)$$

The smoothed value is yielded by $O(n)$ at the central point $n{=}0$ and $O(0){=}a_0$. The process above is iterated for each time slot.

C. FISFA Model

In addition to using the SG filter in the data preprocessing stage, FISFA combines the FEDformer model and the FECAM block. The details of the two modules are given below.

1) FEDformer: FEDformer [23] follows the encoder-decoder structure, which includes four modules: Frequency-Enhanced Block (FEB), Frequency-Enhanced Attention (FEA), Mixture of Experts Decomposition block (MOEDecomp), and a feed-forward layer. The encoder is defined as χ_{en}^{l}=Encoder(χ_{en}^{l-1}). χ_{en}^{l} is the output in the encoder layer l, $l\in\{1,...,N\}$. N denotes the number of layers in encoder. $\chi_{en}^{0}\in\mathbb{R}^{I\times D}$ denotes the embedded result of the historical time series. D denotes the dimension of the embedding layer. Encoder($\cdot$) is defined as:

$$\begin{aligned}
S_{en}^{l,1}, _ &= \text{MOEDecomp}(\text{FEB}(\chi_{en}^{l-1})+\chi_{en}^{l-1})\\
S_{en}^{l,2}, _ &= \text{MOEDecomp}(\text{FeedForward}(S_{en}^{l,1})+S_{en}^{l,1})\\
\chi_{en}^{l} &= S_{en}^{l,2}.
\end{aligned} \tag{4}$$

where $S_{en}^{l,i}, i\in\{1,2\}$ is the seasonal component after decomposition block i in layer l. The symbol _ means the eliminated trend part. FEB is implemented based on Discrete Fourier Transform (DFT). It can effectively replace the self-attention block in traditional transformer models. Given a series of numbers, X_n, in the time domain, FEB processes it with the Fourier transform and the inverse Fourier transform. In this way, the conversion between the time domain and the frequency domain is realized. X_ς is a complex series in the frequency domain, and $1\leq\varsigma\leq\hat{\varsigma}$ where $\hat{\varsigma}$ denotes the sequence length of complex numbers in the frequency domain. X_n is the value of time point n (n=$0,1,\ldots,t-1$) in the time series of real numbers in the time domain. X_ς and X_n are defined as:

$$X_\varsigma = \sum_{n=0}^{t-1} X_n e^{-i\varsigma\omega n} \tag{5}$$

$$X_n = \sum_{\varsigma=0}^{\hat{\varsigma}-1} X_\varsigma e^{i\varsigma\omega n} \tag{6}$$

where i denotes the imaginary unit and ω denotes the angular frequency.

The output of decoder layer l includes $\mathit{\Gamma}_{de}^{l}$ and χ_{de}^{l}, which are the results of Decoder($\chi_{en}^{l-1}, \mathit{\Gamma}_{de}^{l-1}$). The Decoder($\cdot$) is defined as:

$$\begin{aligned}
S_{de}^{l,1}, \mathit{\Gamma}_{de}^{l,1} &= \text{MOEDecomp}(\text{FEB}(\chi_{de}^{l-1})+\chi_{de}^{l-1})\\
S_{de}^{l,2}, \mathit{\Gamma}_{de}^{l,2} &= \text{MOEDecomp}(\text{FEA}(S_{de}^{l,1}, \chi_{de}^{N})+S_{de}^{l,1})\\
S_{de}^{l,3}, \mathit{\Gamma}_{de}^{l,3} &= \text{MOEDecomp}(\text{FeedForward}(S_{de}^{l,2})+S_{de}^{l,2})\\
\chi_{de}^{l} &= S_{de}^{l,3}\\
\mathit{\Gamma}_{de}^{l} &= \mathit{\Gamma}_{de}^{l-1}+W_{l,1}\mathit{\Gamma}_{de}^{l,1}+W_{l,2}\mathit{\Gamma}_{de}^{l,2}+W_{l,3}\mathit{\Gamma}_{de}^{l,3}.
\end{aligned} \tag{7}$$

where $S_{de}^{l,i}$ and $\mathit{\Gamma}_{de}^{l,i}, i\in\{1,2,3\}$, denote the seasonal and trend components after the decompoition block i in layer l, respectively. $W_{l,i}$ is the projector. FEA is also implemented based on DFT with an attention mechanism. It can replace the cross-attention block. MOEDecomp is a progressive decomposition architecture. Traditional fixed-window averaging pooling struggles to extract trends effectively. Thus, it comprises a set of average filters with varying sizes designed to extract multiple trend components in the input signal. Additionally, it utilizes many data-dependent weights to merge these components as the ultimate trend, $\acute{X}_{trend}$, which is a time series decomposed by the MOEDecomp operation and $\acute{X}_{trend}$ includes $\mathit{\Gamma}_{de}^{l,1}$, $\mathit{\Gamma}_{de}^{l,2}$, and $\mathit{\Gamma}_{de}^{l,3}$. $\acute{X}_{trend}$ is defined as:

$$\acute{X}_{trend} = \text{Softmax}(\text{Linear}(\psi)G(\psi)) \tag{8}$$

where ψ denotes the input of the MOEDecomp operation in (7), Linear(ψ) denotes the linear operation on ψ, $G(\psi)$ denotes the average pooling filtering operation on ψ, and Softmax(Linear(ψ)) is the weighted result for mixing extracted trends, which is the final $\acute{X}_{trend}$.

Finally, the prediction results are obtained by the sum of two decomposed components, *i.e.*, $W\chi_{de}^{M}+\mathit{\Gamma}_{de}^{M}$. M denotes the number of layers in the decoder. W is used to convert the seasonal component χ_{de}^{M} to the target dimension.

2) FECAM block: Current methods mainly adopt the Fourier transform to extract frequency information from the time series. If the values of the two ends of the sequence differ greatly, the Fourier transform introduces high-frequency noise. It causes an error for boundary information called the Gibbs phenomenon. To address this problem, FECAM [24] based on discrete cosine transform (DCT) is proposed. FECAM adopts DCT to extract the frequency information. This method avoids the Gibbs issue and the operation of inverse transformation. The features are divided by FECAM into d sub-groups, *i.e.*, $[\kappa_1, \kappa_2, \ldots, \kappa_d]$ according to the dimension of the input. Each sub-group is processed by the component of DCT from low frequency to high one. F^z denotes the zth frequency channel vector, which is obtained as:

$$F^z = \text{DCT}_j(\kappa^z), z\in\{0,1,\ldots,d\}. \tag{9}$$

where DCT$_j$ denotes the frequency component corresponding to κ^z. The stack operation obtains the complete frequency channel vector F.

$$F = \text{stack}(F^0, F^1, \ldots, F^{d-1}). \tag{10}$$

Finally, critical temporal information from the frequency domain of each channel feature is obtained. Therefore, as illustrated in Fig. 1, the filter of SG is adopted to denoise the raw data. Then, we use the FEDformer model to analyze the context information in the time series. Besides, we add a FEACM module between the encoder and the decoder. It additionally boosts the capacity to extract the frequency information in the time series.

D. GSPSO

Deep learning-based models typically have many hyperparameters that highly affect the performance of the FISFA. For example, they involve the number of train epochs, batch size, the layer numbers in the encoder and decoder, learning rate, and dropout rate. Tuning these hyperparameters is a time-consuming task. Particle Swarm Optimizer (PSO) [43], [44] can be used to determine the optimal hyperparameters

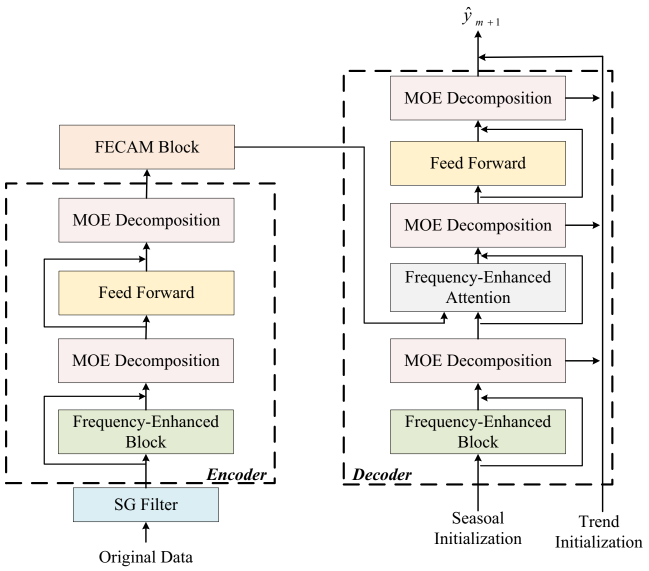

Fig. 1. Structure of FISFA.

effectively. Our work designs an improved version of PSO [45] to accomplish the optimal hyperparameters.

Similar to social behaviors of bird or fish swarm [46], [47], PSO involves a population of particles moving through a search space. These particles adjust positions based on their individual experiences and those of neighboring particles to find the optimal solution, and therefore, they can converge quickly. However, it often converges towards local optima when applied to address constrained problems with sophisticated solution spaces. Besides, SA employs the rule of Metropolis acceptance, thus enabling moves that might deteriorate the search. This capability allows SA to converge towards the global optima using the optimal cooling rate. Nevertheless, it is worth noting that SA converges slowly. Besides, in GA, genetic operations yield diverse individuals, enhancing the global search capability. Therefore, GSPSO combines the strengths of three algorithms by integrating the rule of Metropolis acceptance, genetic operations, and PSO.

Algorithm 1 exhibits GSPSO's pseudo-codes. Line 1 randomly sets the position and velocity of each particle. Line 2 calculates each particle's fitness value $\breve{\phi}$. Line 3 updates $\breve{x}_i$ and $\hat{x}$. $\breve{x}_i$ means particle i's locally optimal position. $\hat{x}$ means the globally optimal position in the population. Line 4 sets GA's mutation possibility θ_5, SA's initial temperature θ_4^1 and its cooling rate θ_7, and PSO's parameters including $\breve{\theta}_2$, $\hat{\theta}_2$, θ_3, $\hat{\theta}_1$, $\breve{\theta}_1$, $\hat{\theta}_6$, $\hat{g}$, and $|x|$. $\breve{\theta}_2$ means an individual coefficient. $\hat{\theta}_2$ means a social acceleration coefficient. θ_3 means the coefficient of acceleration for a superior particle. $\breve{\theta}_1$ denotes the inertia weight. $\hat{g}$ denotes the total iteration number. $\hat{\theta}_6$ means the percentage of particles with identical $\breve{\phi}$. $|x|$ is the size of population. Line 6 means the while loop stops if $g>\hat{g}$ or $\theta_6>\hat{\theta}_6$. Line 7 executes GA's crossover on $\breve{x}_i$ and $\hat{x}$ with the single-point crossover to yield an offspring $\breve{x}_i$. Line 8 executes GA's mutation on each bit of offspring $\breve{x}_i$ with a probability θ_5.

Algorithm 1 GSPSO

1: Initialize particle information randomly
2: Update $\breve{\phi}$ of particles
3: Select $\breve{x}_i$ and $\hat{x}$
4: Set GA's θ_5, SA's θ_4^1 and θ_7, and PSO's parameters, including $\breve{\theta}_2$, $\hat{\theta}_2$, θ_3, $\hat{\theta}_1$, $\breve{\theta}_1$, $\hat{\theta}_6$, $\hat{g}$, and $|x|$
5: $g \leftarrow 1$
6: **while** $\theta_6 \leq \hat{\theta}_6$ and $g \leq \hat{g}$ **do**
7: Execute crossover of GA on $\breve{x}_i$ and $\hat{x}$ to yield an offspring $\breve{x}_i$
8: Execute mutation of GA on each bit of $\breve{x}_i$ with a probability θ_5
9: Execute selection of GA for particle i
10: Calculate velocities of particles with (11)
11: Calculate positions of particles with (12) and (13)
12: Calculate $\breve{\phi}$ of particles
13: Change $\breve{x}_i$ of particle i, and $\hat{x}$
14: $\theta_4^g \leftarrow \theta_4^g \cdot \theta_7$
15: $\theta_1 \leftarrow \left(\hat{\theta}_1 - \breve{\theta}_1\right) \cdot \frac{\hat{g}-g}{\hat{g}} + \breve{\theta}_1$
16: Update θ_6 of particles with the same $\breve{\phi}$
17: $g \leftarrow g+1$
18: **end while**
19: **return** $\hat{x}$

Line 9 executes GA's selection to specify $\breve{x}_i$ or $\dot{x}_i$ is chosen. $\dot{x}_i$ denotes the position of a superior particle for particle i. Line 10 updates the velocity of each particle with (11).

$$v_i = \theta_1 v_i + \theta_3 w_3 (\dot{x}_i - x_i^g) \tag{11}$$

where v_i is the velocity of each particle i. x_i^g means particle i's position in iteration g. Line 11 changes the position of each particle with (12) and (13). More specifically, if $\tilde{\phi}(x_i^{g+1}) \leq \tilde{\phi}(x_i^g)$, x_i^{g+1} is selected; otherwise, it is conditionally selected if (13) is met.

$$x_i^{g+1} = x_i^g + v_i \tag{12}$$

$$e^{\left(\frac{\tilde{\phi}(x_i^{g+1}) - \tilde{\phi}(x_i^g)}{\theta_4^g}\right)} > w_4 \tag{13}$$

where w_4 is a constant randomly selected in $(0,1)$. θ_4^g is current temperature in iteration g.

Line 12 calculates each particle's fitness value $\breve{\phi}$. Line 13 changes particle i's locally optimal position $\breve{x}_i$ and the population's globally optimal position $\hat{x}$. Besides, θ_4^1 is the initial temperature, and θ_7 is its cooling rate. Line 14 reduces temperature by θ_7. $\hat{\theta}_1$ and $\breve{\theta}_1$ are upper and lower bounds of inertia weight θ_1. Line 15 linearly decreases θ_1 from $\hat{\theta}_1$ to $\breve{\theta}_1$. Line 16 calculates percentage θ_6 of particles with identical $\breve{\phi}$. Line 19 returns $\hat{x}$, including the final setting of hyperparameters. Fig. 2 shows the flowchart of GSPSO to optimize the setting of several hyperparameters of FISFA, yielding the optimal hyperparameter setting that minimizes the training loss.

Moreover, GSPSO revises the optimal local position for each particle and updates the globally optimal position within

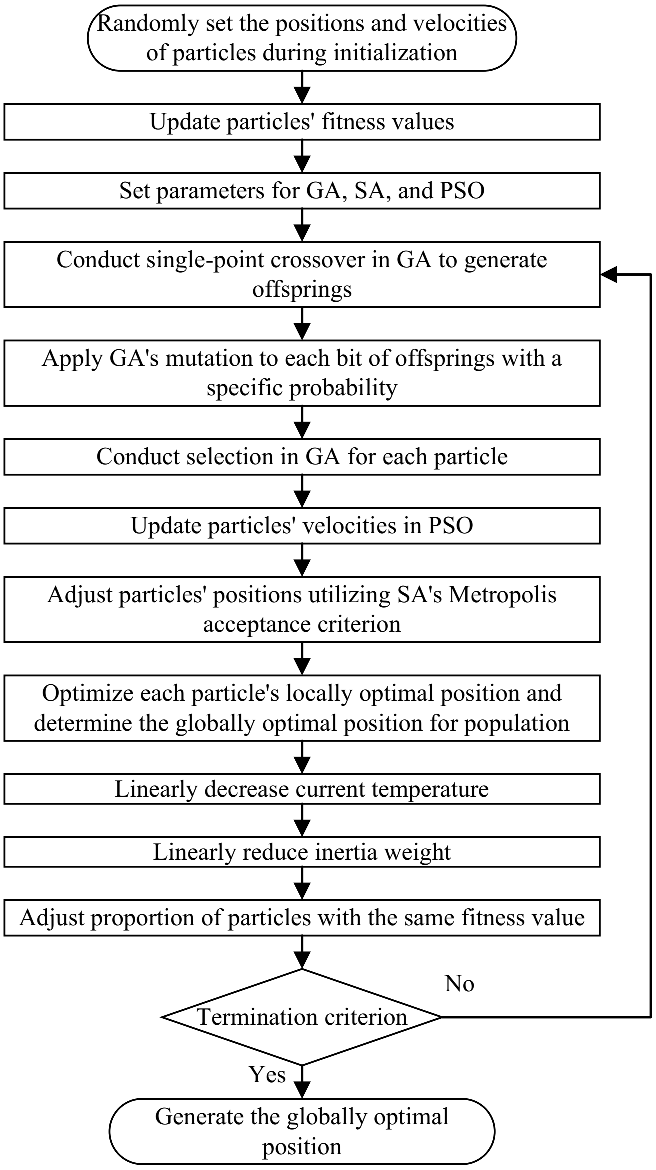

Fig. 2. Flowchart of GSPSO.

the whole population. Additionally, the inertia weight and current temperature decrease linearly. Eventually, it adjusts the proportion of particles sharing identical fitness values and determines whether the termination criterion is satisfied. If it is met, the globally optimal solution is attained; otherwise, the single-point crossover of GA and the following procedures continue to iterate until the termination criterion is satisfied.

E. Complexity Analysis

The most time-consuming operation of FISFA lies in the training stage. t is also the length of the input series. The time complexity $O(t^2)$ of Transformer mainly comes from the self-attention mechanism. FISFA replaces the self-attention mechanism with the discrete Fourier transform with a time complexity $O(t(\log t))$ [23] for the frequency domain feature extraction. Meanwhile, GSPSO performs $\hat{g}$ iterations. Therefore, the time complexity of FISFA is $O(\hat{g}t(\log t))$.

IV. PERFORMANCE EVALUATION

We assess FISFA with realistic datasets and compare its performance with transformer-based prediction models and other traditional methods.

A. Dataset and Experimental Setup

To confirm the efficacy of FISFA, we adopt two heterogeneous real-world datasets collected from Alibaba and Google clusters, respectively. The former dataset includes runtime information on machine resource usage from 4,000 machines in eight days. The log of Cluster-trace-v2018 of Alibaba provides seven cluster data tables. The machine usage table includes CPU utilization, memory utilization, memory bandwidth, cache miss per thousand instructions, incoming and outgoing network traffic, and disk I/O. We select five key resource metrics for the prediction. The time interval is one minute. Tasks are categorized based on the machines with IDs 649 and 1932. Finally, the resource usage time series is obtained and shown in Figs. 3 and 4. Google cluster traces provide information about CDCs in eight regions in May 2019. We choose one dataset with a timezone located in New York, USA. It includes information about CPU usage and alloc sets (shared resource reservations used by jobs). We split 31 days into 14,880 3-minute time slots. Finally, the time series of CPU and memory resources requested for the instance are shown in Fig. 5.

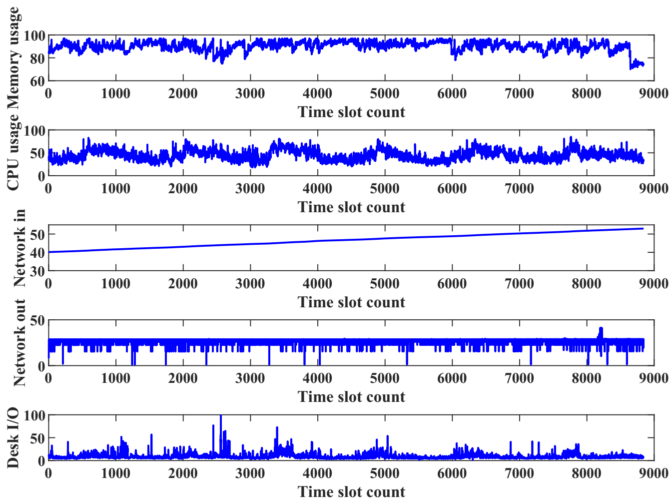

Fig. 3. Resource usage time series of machine ID 649 in the Alibaba cluster dataset

B. Evaluation Metrics

We utilize three metrics including *i.e.*, Root Mean Square Error (RMSE) [48], Mean Absolute Percentage Error (MAPE)

TABLE II
COMPARISON OF DIFFERENT COMBINATIONS OF HYPERPARAMETERS

Combinations	Layer # in encoder (α)	Layer # in decoder (β)	Batch size (γ)	RSME	MAE	MAPE
Combination 1	1	1	32	2.35794	1.38672	0.07374
Combination 2	2	1	32	2.34254	1.37809	0.07331
Combination 3	2	1	16	2.35916	1.39187	0.07390
Combination by GSPSO	1	2	16	**2.33819**	**1.37100**	**0.07325**

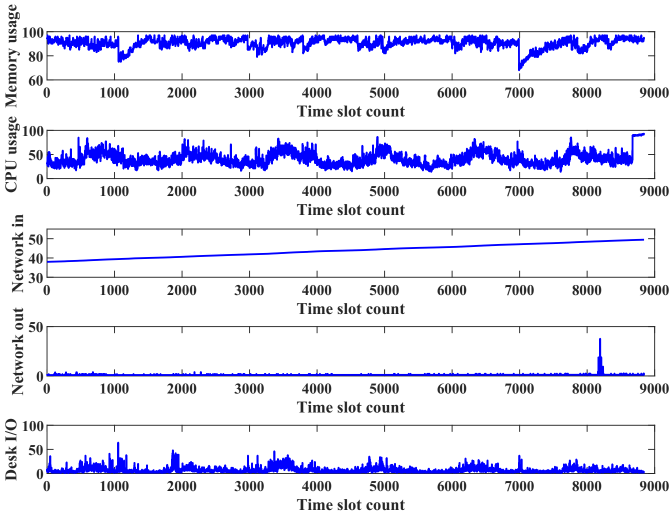

Fig. 4. Resource usage time series of machine ID 1932 in the Alibaba cluster dataset

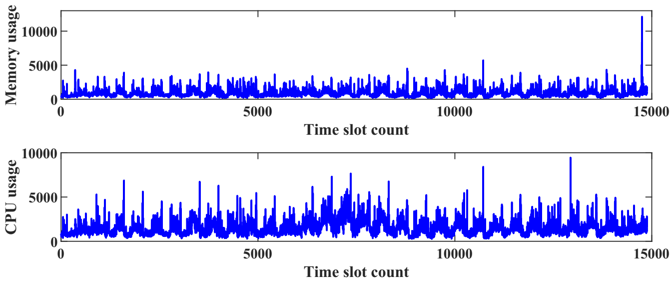

Fig. 5. Resource usage time series of the Google cluster dataset

[49], and Mean Absolute Error (MAE) [50]. They are calculated as follows:

$$\begin{aligned} &\text{RMSE}=\sqrt{\frac{1}{m}\sum_{t=1}^{m}(y_t-\hat{y}_t)^2} \\ &\text{MAPE}=\frac{100\%}{m}\sum_{t=1}^{m}\left|\frac{y_t-\hat{y}_t}{y_t}\right| \\ &\text{MAE}=\frac{1}{m}\sum_{t=1}^{m}|y_t-\hat{y}_t|. \end{aligned} \tag{14}$$

where n is the sample number, $\hat{y}_t$ is the average of the ground truth values, and y_t is the predicted result in time slot t.

C. Hyperparameter Setting

To determine the optimal hyperparameter setting, comprehensive experiments are conducted systemically. Table III displays the final hyperparameter tuning results. The rate of learning is 0.001. The model dimension is 256. The function of loss is Mean Square Error (MSE), and the early stopping patience is 9. Besides, we utilize GSPSO to optimize several key hyperparameters in our model. Three crucial hyperparameters are chosen, including the layer number of encoder (α), the layer number of decoder (β), and the batch size (γ). Finally, α, β, and γ are set to 1, 2, and 16, respectively. Table II illustrates experimental results after selecting four different combinations of hyperparameters. The results show that the hyperparameter configuration yielded by GSPSO produces the highest prediction accuracy. The parameter configurations for FISFA are outlined in Table III.

TABLE III
SETTING OF FISFA PARAMETERS

Parameters	Values
Dimension of model	256
Learning rate	0.001
Activation	gelu
Layer number in encoder	1
Layer number in decoder	2
Batch size	16
Early stopping patience	9
Loss function	MSE

D. Analysis of Prediction Results

We allocate 70% of the time series for the training, 10% for the validation, and the remaining 20% for the testing. To evaluate FECAM in the prediction, comparison experiments of FEDformers with and without the FECAM block are conducted. Table IV shows the results of three evaluation metrics. The odd and even rows represent metric values for FEDformer and FEDformer with FECAM, respectively. The results prove that the FEDformer with FECAM outperforms its vanilla version.

We choose several benchmark methods to compare our FISFA with its other state-of-the-art peers comprehensively. For example, LSTM is based on the gated cell and is commonly used for time series prediction. However, it suffers from the gradient explosion problem during training and cannot effectively extract the correlation among multi-dimensional data. Informer is an improved transformer model with low time complexity and memory utilization. However, it cannot effectively extract frequency domain features.

Furthermore, Tables V–VII show the performance comparison between FISFA and various prediction methods including LSTM and transformer-based models, *e.g.*, transformer and

TABLE IV
COMPARISON OF FEDFORMER AND FEDFORMER WITH FECAM

Dimension of model	RMSE	MAE	MAPE
8	3.11518	1.79656	0.09408
	3.11**257**	1.79**477**	0.09**400**
16	3.07927	1.78386	0.08947
	3.07**812**	1.78**276**	0.08943
32	3.03130	1.72264	0.09138
	3.03**113**	1.72**250**	0.09138
64	2.99807	1.69626	0.09013
	2.99**768**	1.69**571**	0.09**008**
128	2.99799	1.69064	0.08947
	2.99805	1.69**059**	0.08947
256	2.99309	1.68770	0.08900
	2.**98965**	1.68**498**	0.08**886**

Informer. The abbreviation FEC signifies that forecasting models employ FECAM. SG- means thatthe SG filter is adopted. Table V shows the transformer-based models achieve higher performance than LSTM in the multi-dimension prediction. FECAM and the SG filter improve the evaluation metric values, and FISFA achieves the highest accuracy among all these methods.

TABLE V
PERFORMANCE COMPARISON OF ALL METHODS WITH THE DATASET OF MACHINE ID 649 FROM ALIBABA

Methods	RMSE	MAE	MAPE
LSTM	3.46993	2.26280	0.10308
Transformer	3.09399	1.89245	0.10084
Informer	3.19903	2.02076	0.10897
FEDformer	2.99309	1.68770	0.08900
Transformer+FEC	3.08164	1.89849	0.10042
Informer+FEC	3.19222	2.00831	0.10858
FEDformer+FEC	2.98965	1.68498	0.08886
SG-LSTM	3.43238	2.22098	0.10182
SG-Transformer	*2.40196*	*1.45422*	*0.07335*
SG-Informer	2.47797	1.54587	0.07423
FISFA	**2.32237**	**1.34573**	**0.07271**

TABLE VI
PERFORMANCE COMPARISON OF ALL METHODS WITH THE DATASET OF MACHINE ID 1932 FROM ALIBABA

Methods	RMSE	MAE	MAPE
LSTM	3.97746	2.23827	0.27784
Transformer	3.37595	1.77665	0.10875
Informer	3.53577	1.85022	0.11172
FEDformer	3.33543	1.39523	0.11575
Transformer+FEC	3.41701	1.79651	0.11500
Informer+FEC	3.33480	1.78247	0.10704
FEDformer+FEC	3.31267	1.39752	0.11484
SG-LSTM	3.95284	2.21583	0.27527
SG-Transformer	*2.46992*	*1.28261*	*0.09220*
SG-Informer	2.51991	1.33650	0.08498
FISFA	**2.29162**	**1.01012**	**0.08320**

Table VIII shows the ablation studies of FISFA with three methods. It is evident that the addition of each method can bring improvement to the prediction. Fig. 6 shows ground truth values and the predicted ones of RAM usage, CPU usage, Network in, Network out, and Desk I/O, respectively. Fig. 7 compares loss values of Transformer, Informer, Autoformer, FEDformer, and FEDformer with FECAM for the resource

TABLE VII
PERFORMANCE COMPARISON OF ALL METHODS WITH THE GOOGLE DATASET

Methods	RMSE	MAE	MAPE
LSTM	491.185	297.653	0.27746
Transformer	481.125	299.474	0.27375
Informer	488.582	306.436	0.27840
FEDformer	476.954	296.782	0.26898
Transformer+FEC	482.027	300.138	0.27428
Informer+FEC	484.144	301.987	0.27642
FEDformer+FEC	476.818	295.825	0.26754
SG-LSTM	396.026	242.718	0.23827
SG-Transformer	400.740	*249.598*	*0.22345*
SG-Informer	*398.055*	250.062	0.22784
FISFA	**387.199**	**239.265**	**0.21533**

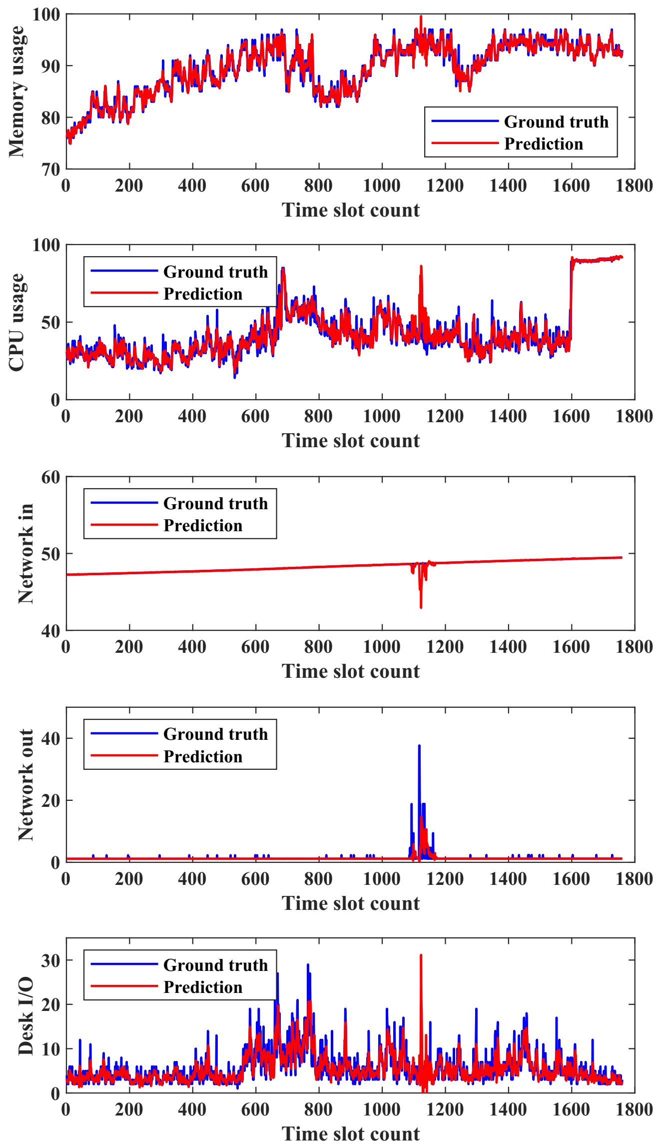

Fig. 6. Prediction curves of resource usage time series of machine ID 1932

TABLE VIII
ABLATION STUDIES OF FISFA WITH THREE METHODS

Methods	RMSE	MAE	MAPE
w/o SG filter	2.98965	1.68498	0.08886
w/o FECAM	2.32727	1.34451	0.07337
w/o GSPSO	2.35916	1.39187	0.07390
FISFA	**2.32237**	**1.34573**	**0.07271**

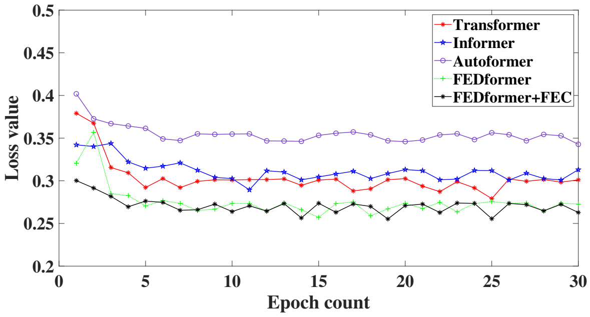

Fig. 7. Loss values of different methods for resource usage time series of machine ID 1932.

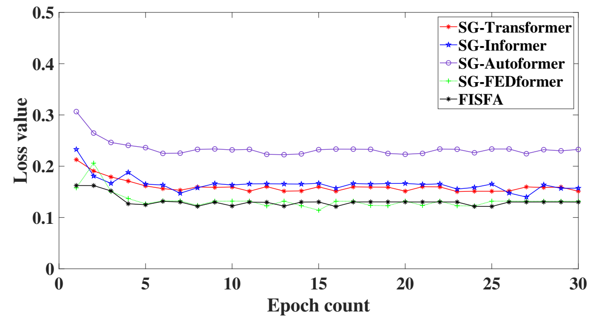

Fig. 8. Loss values of different methods after adding the SG filter.

usage time series of machine ID 1932, respectively. Fig. 8 shows the loss values of different methods after adding the SG filter. After iteration 10, it is evident that FISFA's loss values are comparatively smaller than those of other models. This demonstrates that FISFA possesses superior modeling capabilities compared with other transformer variants. Consequently, FISFA outperforms other benchmark methods given the same setting.

V. CONCLUSIONS AND FUTURE WORK

Current cloud providers face a critical but challenging problem of accurately predicting computing resource usage in cloud data centers. Resource usage series is often multi-dimensional and volatile. Each series is characterized by different trends, increasing the difficulty of forecasting. Most current forecasting methods cannot effectively extract correlations among multiple series and frequency domain information. This work proposes a Forecasting method based on the Integration of a Savitzky-Golay (SG) filter, a Frequency Enhanced Decomposed Transformer (FEDformer) model, and a Frequency-Enhanced channel Attention mechanism (FECAM), named FISFA for short, for forecasting the multi-dimensional computing resource usage series. FISFA initially adopts the SG filter to accomplish better noise reduction. It designs a FEDformer model with a frequency-enhanced channel attention mechanism to investigate key patterns from resource usage time series in the frequency domain. In addition, a hybrid meta-heuristic optimization algorithm called genetic simulated annealing-based particle swarm optimizer is proposed to optimize key hyperparameters of FISFA. At last, experiments with two heterogeneous real-world datasets from Alibaba and Google demonstrate that FISFA achieves superior forecasting accuracy than its baseline peers. Against LSTM, Transformer, and Informer, our prediction accuracy is improved by 32.14%, 25.49%, and 27.71%, respectively.

As part of future work, we will apply FISFA to more diverse real-world workload datasets. We also plan to incorporate novel spatial-temporal graph convolution networks to enhance performance. In addition, we plan to employ meta-learning to provide beneficial guidance on learning a more generalized and adaptive model for predicting resource usage in cloud data centers.

REFERENCES

[1] A. Jayanetti, S. Halgamuge, and R. Buyya, "Multi-Agent Deep Reinforcement Learning Framework for Renewable Energy-Aware Workflow Scheduling on Distributed Cloud Data Centers," *IEEE Transactions on Parallel and Distributed Systems*, vol. 35, no. 4, pp. 604–615, Apr. 2024.
[2] J. Bi, H. Yuan, J. Zhang, and M. Zhou, "Green Energy Forecast-Based Bi-Objective Scheduling of Tasks Across Distributed Clouds," *IEEE Transactions on Sustainable Computing*, vol. 7, no. 3, pp. 619–630, Jul. 2022.
[3] Y. Xia, M. Zhou, X. Luo, Q. Zhu, J. Li, and Y. Huang, "Stochastic Modeling and Quality Evaluation of Infrastructure-as-a-Service Clouds," *IEEE Transactions on Automation Science and Engineering*, vol. 12, no. 1, pp. 162–170, Jan. 2015.
[4] H. Yuan, J. Bi, and M. Zhou, "Profit-Sensitive Spatial Scheduling of Multi-Application Tasks in Distributed Green Clouds," *IEEE Transactions on Automation Science and Engineering*, vol. 17, no. 3, pp. 1097–1106, Jul. 2020.
[5] Q. Peng, C. Wu, Y. Xia, Y. Ma, X. Wang and N. Jiang, "DoSRA: A Decentralized Approach to Online Edge Task Scheduling and Resource Allocation," *IEEE Internet of Things Journal*, vol. 9, no. 6, pp. 4677–4692, Mar. 2022.
[6] J. Bi, H. Yuan, K. Zhang, and M. Zhou, "Energy-Minimized Partial Computation Offloading for Delay-Sensitive Applications in Heterogeneous Edge Networks," *IEEE Transactions on Emerging Topics in Computing*, vol. 10, no. 4, pp. 1941–1954, Dec. 2022.
[7] H. Yuan, J. Bi, and M. Zhou, "Geography-Aware Task Scheduling for Profit Maximization in Distributed Green Data Centers," *IEEE Transactions on Cloud Computing*, vol. 10, no. 3, pp. 1864–1874, Sept. 2022.
[8] J. Bi, H. Yuan, J. Zhang, and M. Zhou, "Green Energy Forecast-Based Bi-Objective Scheduling of Tasks Across Distributed Clouds," *IEEE Transactions on Sustainable Computing*, vol. 7, no. 3, pp. 619–630, Sept. 2022.
[9] T. Long, P. Chen, Y. Xia, Y. Ma, X. Sun, J. Zhao, Y. Lyu, "A Deep Deterministic Policy Gradient-based Method for Enforcing Service Fault-tolerance in MEC," *Chinese Journal of Electronics*, vol. 33, no. 5, pp. 1–11, 2023.
[10] J. Guo, Z. Chang, S. Wang, H. Ding, Y. Feng, L. Mao, and Y. Bao, "Who Limits the Resource Efficiency of My Datacenter: An Analysis of Alibaba Datacenter Traces," *2019 IEEE/ACM 27th IEEE/ACM International Symposium on Quality of Service*, pp. 1–10, Guangzhou, China, 2019.

[11] S. Tuli, S. S. Gill, P. Garraghan, R. Buyya, G. Casale, and N. R. Jennings, "START: Straggler Prediction and Mitigation for Cloud Computing Environments Using Encoder LSTM Networks," *IEEE Transactions on Services Computing*, vol. 16, no. 1, pp. 615–627, Feb. 2023.

[12] X. Tang, X. Liao, J. Zheng, and X. Yang, "Energy Efficient Job Scheduling with Workload Prediction on Cloud Data Center," *Cluster Computing*, vol. 21, pp. 1581–1593. Feb. 2018.

[13] B. Fei, X. Zhu, D. Liu, J. Chen, W. Bao, and L. Liu, "Elastic Resource Provisioning Using Data Clustering in Cloud Service Platform," *IEEE Transactions on Services Computing*, vol. 15, no. 3, pp. 1578–1591, May 2022.

[14] N. Hogade and S. Pasricha, "A Survey on Machine Learning for Geo-Distributed Cloud Data Center Management," *IEEE Transactions on Sustainable Computing*, vol. 8, no. 1, pp. 15–31, Jan. 2023.

[15] Z. Xing, Y. He, X. Wang, K. Shao, and J. Duan, "VMD-IARIMA-Based Time-Series Forecasting Model and its Application in Dissolved Gas Analysis," *IEEE Transactions on Dielectrics and Electrical Insulation*, vol. 30, no. 2, pp. 802–811, Apr. 2023.

[16] M. Hossain, E. Gray, J. Lu, M. Islam, M. Alam, R. Chakrabortty, and H. Pota, "Optimized Forecasting Model to Improve the Accuracy of Very Short-Term Wind Power Prediction," *IEEE Transactions on Industrial Informatics*, vol. 19, no. 10, pp. 10145–10159, Oct. 2023.

[17] S. Gupta, A. D. Dileep, and T. A. Gonsalves, "Online Sparse BLSTM Models for Resource Usage Prediction in Cloud Datacentres," *IEEE Transactions on Network and Service Management*, vol. 17, no. 4, pp. 2335–2349, Dec. 2020.

[18] A. Zollanvari, K. Kunanbayev, S. Bitaghsir, and M. Bagheri, "Transformer Fault Prognosis Using Deep Recurrent Neural Network Over Vibration Signals," *IEEE Transactions on Instrumentation and Measurement*, vol. 70, pp. 1–11, Sept. 2021.

[19] Y. Yu, G. Hu, C. Liu, J. Xiong, and Z. Wu, "Prediction of Solar Irradiance One Hour Ahead Based on Quantum Long Short-Term Memory Network," *IEEE Transactions on Quantum Engineering*, vol. 4, pp. 1–15, Apr. 2023.

[20] S. Saha, A. Haque, and G. Sidebottom, "Analyzing the Impact of Outlier Data Points on Multi-Step Internet Traffic Prediction Using Deep Sequence Models," *IEEE Transactions on Network and Service Management*, vol. 20, no. 2, pp. 1345–1362, Jun. 2023.

[21] Y. Xie, J. Niu, Y. Zhang, and F. Ren, "Multisize Patched Spatial-Temporal Transformer Network for Short- and Long-Term Crowd Flow Prediction," *IEEE Transactions on Intelligent Transportation Systems*, vol. 23, no. 11, pp. 21548–21568, Nov. 2022.

[22] A. Savitzky and M. Golay, "Smoothing and Differentiation of Data by Simplified Least Squares Procedures," *Analytical Chemistry*, vol. 36, pp. 1627–1639, Jul. 1964.

[23] T. Zhou, Z. Ma, Q. Wen, X. Wang, L. Sun, and Rong Jin, "FEDformer: Frequency Enhanced Decomposed Transformer for Long-term Series Forecasting," *Proceedings of the 39th International Conference on Machine Learning*, pp. 1–19, Baltimore, Maryland, USA, 2022.

[24] M. Jiang, P. Zeng, K. Wang, H. Liu, W. Chen, and Haoran Liu, "FECAM: Frequency Enhanced Channel Attention Mechanism for Time Series Forecasting," *Advanced Engineering Informatics*, vol. 58, pp. 1–11, Oct. 2023.

[25] C. Yang and Z. Pei, "Long-Short Term Spatio-Temporal Aggregation for Trajectory Prediction," *IEEE Transactions on Intelligent Transportation Systems*, vol. 24, no. 4, pp. 4114–4126, Apr. 2023.

[26] X. Chen, H. Zhang, F. Zhao, Y. Cai, H. Wang, and Q. Ye, "Vehicle Trajectory Prediction Based on Intention-Aware Non-Autoregressive Transformer With Multi-Attention Learning for Internet of Vehicles," *IEEE Transactions on Instrumentation and Measurement*, vol. 71, pp. 1–12, 2022.

[27] H. Shen, Z. Wang, X. Zhou, M. Lamantia, K. Yang, P. Chen, and J Wang, "Electric Vehicle Velocity and Energy Consumption Predictions Using Transformer and Markov-Chain Monte Carlo," *IEEE Transactions on Transportation Electrification*, vol. 8, no. 3, pp. 3836–3847, Sept. 2022.

[28] P. Xie, M. Ma, T. Li, S. Ji, S. Du, Z. Yu, and J Zhang, "Spatio-Temporal Dynamic Graph Relation Learning for Urban Metro Flow Prediction," *IEEE Transactions on Knowledge and Data Engineering*, vol. 35, no. 10, pp. 9973–9984, Oct. 2023.

[29] T. W. Gyeera, A. J. H. Simons, and M. Stannett, "Regression Analysis of Predictions and Forecasts of Cloud Data Center KPIs Using the Boosted Decision Tree Algorithm," *IEEE Transactions on Big Data*, vol. 9, no. 4, pp. 1071–1085, Aug. 2023.

[30] Y. Zhang, X. Shi, S. Zhang, and A. Abraham, "An XGBoost-Based Lane Change Prediction on Time Series Data Using Feature Engineering for Autopilot Vehicles," *IEEE Transactions on Intelligent Transportation Systems*, vol. 23, no. 10, pp. 19187–19200, Oct. 2022.

[31] B. Feng, Z. Ding, and C. Jiang, "FAST: A Forecasting Model with Adaptive Sliding Window and Time Locality Integration for Dynamic Cloud Workloads," *IEEE Transactions on Services Computing*, vol. 16, no. 2, pp. 1184–1197, Mar. 2023.

[32] F. Shen and R. Yan, "A New Intermediate-Domain SVM-Based Transfer Model for Rolling Bearing RUL Prediction," *IEEE/ASME Transactions on Mechatronics*, vol. 27, no. 3, pp. 1357–1369, Jun. 2022.

[33] N. Wang and J. Y. Li, "Efficient Multi-Channel Thermal Monitoring and Temperature Prediction Based on Improved Linear Regression," *IEEE Transactions on Instrumentation and Measurement*, vol. 71, pp. 1–9, Dec. 2022.

[34] I. K. Kim, W. Wang, Y. Qi, and M. Humphrey, "Forecasting Cloud Application Workloads With CloudInsight for Predictive Resource Management," *IEEE Transactions on Cloud Computing*, vol. 10, no. 3, pp. 1848–1863, Jul. 2022.

[35] M. Kumar, A. Kishor, J. K. Samariya, and A. Y. Zomaya, "An Autonomic Workload Prediction and Resource Allocation Framework for Fog-Enabled Industrial IoT," *IEEE Internet of Things Journal*, vol. 10, no. 11, pp. 9513–9522, Jun. 2023.

[36] Y. Li , L. Song, S. zhang, A. Komandur, and N. Lu , "A TCN-Based Hybrid Forecasting Framework for Hours-Ahead Utility-Scale PV Forecasting," *IEEE Transactions on Smart Grid*, vol. 14, no. 5, pp. 4073–4085, Sept. 2023.

[37] Z. Wang, Z. Li, H. Pan, G. Liu, Y. Chen, Q. Wu, G. Tyson, and G Cheng, "Large-Scale Measurements and Prediction of DC-WAN Traffic," *IEEE Transactions on Parallel and Distributed Systems*, vol. 34, no. 5, pp. 1390–1405, May 2023.

[38] M. A. P. Putra, A. P. Hermawan, C. I. Nwakanma, D. S. Kim, and J. M. Lee, "FDPR: A Novel Fog Data Prediction and Recovery Using Efficient DL in IoT Networks," *IEEE Internet of Things Journal*, vol. 10, no. 19, pp. 16895–16906, Oct. 2023.

[39] L. Ruan, Y. Bai, S. Li, J. Lv, T. Zhang, L. Xiao, H. Fang, C. Wang, and Y. Xue, "Cloud Workload Turning Points Prediction via Cloud Feature-Enhanced Deep Learning," *IEEE Transactions on Cloud Computing*, vol. 11, no. 2, pp. 1719–1732, Jun. 2023.

[40] R. Zhang, J. Chen, Y. Song, Y. Wen, and C. Peng, "An Effective Transformation-Encoding-Attention Framework for Multivariate Time Series Anomaly Detection in IoT Environment," *Mobile Networks and Applications*, Aug. 2023.

[41] K. Gao, X. Li, B. Chen, L. Hu, J. Liu, R. Du, and Y Li, "Dual Transformer Based Prediction for Lane Change Intentions and Trajectories in Mixed Traffic Environment," *IEEE Transactions on Intelligent Transportation Systems*, vol. 24, no. 6, pp. 6203–6216, Jun. 2023.

[42] Z. Zhang, P. Chen, C. Xing, B. Liu, R. Wang, L. Li, X. Chen, and E Zio, "A Data Augmentation Boosted Dual Informer Framework for the Performance Degradation Prediction of Aero-Engines," *IEEE Sensors Journal*, vol. 23, no. 11, pp. 12018–12030, Jun. 2023.

[43] Q. Ge, C. Guo, H. Jiang, Z. Lu, G. Yao, J. Zhang, and Q. Hua, "Industrial Power Load Forecasting Method Based on Reinforcement Learning and PSO-LSSVM," *IEEE Transactions on Cybernetics*, vol. 52, no. 2, pp. 1112–1124, Feb. 2022.

[44] H. Yan, Y. Qi, Q. Ye, and D. Yu, "Robust Least Squares Twin Support Vector Regression With Adaptive FOA and PSO for Short-Term Traffic Flow Prediction," *IEEE Transactions on Intelligent Transportation Systems*, vol. 23, no. 9, pp. 14542–14556, Sept. 2022.

[45] J. Bi, H. Yuan, S. Duanmu, M. Zhou, and A. Abusorrah, "Energy-Optimized Partial Computation Offloading in Mobile-Edge Computing With Genetic Simulated-Annealing-Based Particle Swarm Optimization," *IEEE Internet of Things Journal*, vol. 8, no. 5, pp. 3774–3785, Mar. 2021.

[46] J. Bi, Z. Wang, H. Yuan, J. Qiao, J. Zhang, and M. Zhou, "Self-adaptive Teaching-learning-based Optimizer with Improved RBF and Sparse Autoencoder for Complex Optimization Problems," *2023 IEEE International Conference on Robotics and Automation*, pp. 7966-7972, London, United Kingdom, 2023.

[47] J. Bi, J. Zhai, H. Yuan, Z. Wang, J. Qiao, J. Zhang, and M. Zhou, "Multi-swarm Genetic Gray Wolf Optimizer with Embedded Autoencoders for High-dimensional Expensive Problems," *2023 IEEE International Conference on Robotics and Automation*, 2023, London, United Kingdom, pp. 7265-7271.

[48] T. Chai and R. Draxler, "Root Mean Square Error (RMSE) or Mean Absolute Error (MAE)? – Arguments Against Avoiding RMSE in the Literature," *Geoscientific Model Development*, vol. 7, pp. 1247–1250, Jun. 2014.

[49] J. Bi, L. Zhang, H. Yuan, and J. Zhang, "Multi-Indicator Water Quality Prediction with Attention-Assisted Bidirectional LSTM and Encoder-Decoder," *Information Sciences*, vol. 625, pp. 65–80, May 2023.

[50] J. Qi, J. Du, S. M. Siniscalchi, X. Ma, and C. H. Lee, "Analyzing Upper Bounds on Mean Absolute Errors for Deep Neural Network-Based Vector-to-Vector Regression," *IEEE Transactions on Signal Processing*, vol. 68, pp. 3411–3422, May 2020.

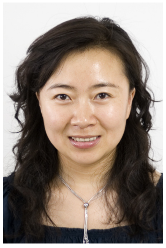

Jing Bi (M'13–SM'16) received her B.S., and Ph.D. degrees in Computer Science from Northeastern University, Shenyang, China, in 2003 and 2011, respectively. From 2013 to 2015, she was a Postdoc researcher in the Department of Automation at Tsinghua University, Beijing, China. From 2018 to 2019, she was a Visiting Research Scholar with the Department of Electrical and Computer Engineering, New Jersey Institute of Technology, Newark, NJ, USA. She is a Professor at the Faculty of Information Technology, School of Software Engineering, Beijing University of Technology, Beijing, China. Her research interests include distributed computing, cloud computing, large-scale data analytics, machine learning, and performance optimization. Dr. Bi received the IBM Fellowship Award, the Best Paper Award at the 17th IEEE International Conference on Networking, Sensing and Control, and the First-Prize Progress Award of the Chinese Institute of Simulation Science and Technology. She is now an Associate Editor of IEEE Transactions on Systems Man and Cybernetics: Systems. She is a senior member of the IEEE.

Haisen Ma is currently a Master's student in the Faculty of Information Technology, School of Software Engineering, Beijing University of Technology, Beijing, China. Before that, he received his B.S. degree in Software Engineering from Zhengzhou University in 2021. His research interests include cloud computing, data centers, big data, time series prediction, machine learning, and deep learning.

Haitao Yuan (S'15–M'17–SM'21) received the Ph.D. degree in Computer Engineering from New Jersey Institute of Technology (NJIT), Newark, NJ, USA in 2020. He is an Associate Professor at the School of Automation Science and Electrical Engineering at Beihang University, Beijing, China. His research interests include cloud computing, edge computing, data centers, big data, machine learning, deep learning, and optimization algorithms. He received the Chinese Government Award for Outstanding Self-Financed Students Abroad, the 2021 Hashimoto Prize from NJIT, and the Best Paper Award in the 17th ICNSC. He serves as an associate editor for Expert Systems with Applications.

Rajkumar Buyya (Fellow, IEEE) is a Redmond Barry Distinguished Professor and Director of the Cloud Computing and Distributed Systems (CLOUDS) Laboratory at the University of Melbourne, Australia. He received a B.E and M.E in Computer Science and Engineering from Mysore and Bangalore Universities in 1992 and 1995, respectively, and a Ph.D. in Computer Science and Software Engineering from Monash University, Melbourne, Australia, in 2002. He was a Future Fellow of the Australian Research Council from 2012 to 2016. He has authored over 850 publications and seven textbooks. He is a highly cited computer science and software engineering author worldwide, with over 146,900 citations and an h-index of 167. Thomson Reuters recognized him as a "Web of Science Highly Cited Researcher" from 2016 to 2021.

Jinhong Yang received the Ph.D. degree in Computer Application Technology from Harbin Engineering University, Harbin, Heilongjiang, China in 2017. She is a Senior Engineer with CSSC Systems Engineering Research Institute in Beijing, China. Her research interests include machine learning, data mining, knowledge reasoning, deep learning, and intelligent optimization. She is a reviewer for Expert Systems With Applications, International Journal of Machine Learning and Cybernetics, *etc*.

Jia Zhang received a Ph.D. degree in computer science from the University of Illinois at Chicago. She is the Cruse C. and Marjorie F. Calahan Centennial Chair in Engineering and a professor of the Department of Computer Science in the Lyle School of Engineering at Southern Methodist University. Her research interests emphasize applying machine learning and information retrieval methods to tackle data science infrastructure problems, with a recent focus on scientific workflows, provenance mining, software discovery, knowledge graphs, and interdisciplinary applications of all these interests in earth science. She is a senior member of the IEEE.

MengChu Zhou (S'88-M'90-SM'93-F'03) received his Ph. D. degree from Rensselaer Polytechnic Institute, Troy, NY in 1990 and then joined New Jersey Institute of Technology where he is now a Distinguished Professor. His interests are Petri nets, automation, Internet of Things, cloud/edge computing, and AI. He has 1000+ publications, including 12 books, 700+ journal papers (600+ in IEEE transactions), 31 patents, and 30 book chapters. He is Fellow of IFAC, AAAS, CAA and NAI.